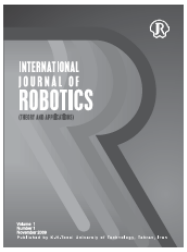

INTERNATIONAL JOURNAL OF ROBOTICS
(THEORY AND APPLICATIONS)
E-mail: IJR@kntu.ac.ir

Tumor Detection and Morphology Assessment in the Liver Tissue Using an Automatic Tactile Robot

S.M.S. Lari[1], A. Mojra[2,*]

[1.] BSc student of Mechanical Engineering, K. N. Toosi University of Technology, Tehran, Iran, smslari@email.kntu.ac.ir
[2.] Assistant Professor of Mechanical Engineering, K. N. Toosi University of Technology, Tehran Iran

ARTICLE INFO

Article history:
Received: August 12, 2015.
Received in revised form:
November 20, 2016.
Accepted: November 22, 2016

Keywords:
Soft tissue
Mechanical stress
Tumor diagnosis
Robotic examination

ABSTRACT

In this paper an automatic examination robot was developed to improve the process of cancer detection, tumor localization and geometrical shape diagnosis. A uniformly distributed compressive load was applied to the top tissue surface and the resultant mechanical stress was measured that was employed for the tumor diagnosis task. The experimental examinations were performed on the soft tissue of the liver. A compression test was used to extract viscoelastic properties of tissue. Viscoelastic coefficients were used in the finite element modeling and the capability of the robotic-assisted tumor detection procedure was verified. Finally to localize the tumor embedded in the tissue, two sinusoidal and step paths were generated which was followed by the robot. The mean errors of path following by the automatic examination robot affirmed the accuracy and the reliability of the Cartesian mechanism in the soft tissue scanning.

1. Introduction

z decisions and improving surgical operations [6,7].Artificial Tactile Sensing (ATS) is a new simulates physical touch in a much more accurate way. Outputs of the system can be used to determine some physical and geometrical properties of an object. ATS coupled with robotic systems can provide exact and quantitative information of what is being touched. This information is called tactile data. A common application in the engineering world is collecting force feedback from sensors, which is widely used in advanced robotic applications, tele-surgery, Minimally Invasive Surgery (MIS), Natural Orifice Transluminal Endoscopic Surgery (NOTES) and other medical and industrial branches [8-14].

Tactile data on the surface may be also employed for estimating abnormalities inside an object. Such ability can be very useful in soft tissue's tumor developing technique which has the advantage of physical examination by being noninvasive. ATS is a method in which a sensory system detection which is embedded inside the tissue. Soft tissue abnormalities are often associated with a local change in tissue's mechanical properties [15]. Physical examination performed by a surgeon is based on such variations [16]. The feasibility of using robotic devices for physical examination is a challenging task which has received much attention during recent years [17,18]. Robotic examination provides quantitative measurements of the tissue's mechanical and geometrical properties for use in medical applications [19]. Parameters achieved by robotic examination can be employed for the estimation of tissue's internal structure and are called haptic parameters. Several robotic devices have been

* Corresponding author,
Tel:+98(21)84063274; Fax: +98(21)88677274; Email: mojra@kntu.ac.ir

introduced and developed for soft tissue examinations.

Carter et al. fabricated a manually operating robot to diagnose diseased human liver tissue from the normal tissue. They reported that the Young's modulus of normal human liver tissue is lower than that of a diseased one [20]. Liu et al. developed a rolling tactile robot mechanism and found that the result of palpation could be applied to identify approximate location, shape, and size of nodules [21]. Chu et al. introduced an exploration strategy for the classification of inclusions by means of a Mitsubishi RV-II robot and a 2-axis force sensor. They measured mechanical behavior of tissue phantoms against normal and lateral examinations and differentiated inclusions from the surrounding tissue [22]. Ayyildiz et al. developed a compression device consisted of a moving shuttle on a power screw driven by a step motor equipped with a contact tactile sensor. The device was used for detection of lumps in a soft tissue [23]. Lee et al. fabricated a tactile sensation imaging device and used it to detect and identify inclusions within soft tissues. The proposed tactile imaging was used for estimation of inclusion diameter within 4.09% and inclusion depth within 7.55% [24]. Most of the robotic devices used for examination and tumor detection are handheld devices and do not have the ability of screening a tissue with high accuracy for tumor localization.

Based on tactile sensing, a number of robotic devices have been introduced to precisely palpate the surface of tissue in many clinical fields. Ottensmeyer et al. developed a minimally invasive instrument (TeMPeST 1-D) to measure the mechanical properties of intra-abdominal organs [25]. Dargahi et al. developed an endoscopic tooth-like tactile sensor which was capable of measuring total applied force on the sensed object as well as the compliance of the tissue/sensed object [26]. Mojra et al. provided a robotic device equipped with a pressure sensor (Robo-Tac-BMI) to characterize the viscoelastic behavior of breast tissue during clinical breast examination [27]. Recently, Ledermann et al. and Büscher et al. investigated the applicability and accuracy of tactile sensing in the surgical procedures [28,29].

In the present study an automatic robot is introduced for exact examination of the liver tissue surface. Haptic parameters are collected on the surface and tumor existence is studied. Numerical analysis is also performed to study capability of robotic ATS in abnormal mass detection and reliability of the robotic device outputs. For exact modeling of the tissue, defining appropriate material properties is a necessity. Many numerical simulations of soft tissue has been performed which suffer from inappropriate material definition. By assuming a homogeneous elastic or hyperelastic behavior for the tissue, outputs cannot be any more reliable [30-36].

It is well known that soft tissues have a viscoelastic or time dependent behavior [37]. Valtorta et al. set the parameters of linear viscoelastic material for bovine liver by dynamic test using a torsional resonator [38]. Shi et al. presented lamb liver tissue linear elastic and viscoelastic FEM using high resolution cone-beam CT images to estimate the changes of volume and shape of surface under small forces. They found that with increasing the load, viscoelastic model become more appropriate [39]. Zhang et al. developed two independent quantitative methods, crawling wave estimator (CRE) and mechanical measurement (MM) for characterization of soft tissue and offered a comparison between two techniques in measuring gelatin phantom, veal liver and human prostate. Experimental results showed the reliability of both CRE and MM methods to investigate the soft tissue viscoelastic properties [40]. Kobayashi et al. validated and developed a nonlinear viscoelastic model of liver for insertion of needle, in which an organ deformation was forecasted and estimated, and the path of needle was marked with deformation of organ [41]. Raghunathan et al. used poroviscoelasticity (PVE) theory to simulate liver biomechanical response in unconfined compression stress relaxation experiments, for rates of variable ramp strain ranging from 0.001 to 0.1s-1. Response of liver was modeled by using ABAQUS, and appropriate parameters were determined using nonlinear least squares algorithms [42].

The main target of this paper was to develop an automatic robot to improve the cancer detection process and localization of tumor. For this purpose a number of mechanical parameters called tactile parameters were extracted from in vitro robotic examination of the tissue surface. The experimental examinations were performed on a lamb liver. In order to precisely scan the sample tissue surface, a sinusoidal path and a step path were defined. The paths were evaluated by a control system and robot accuracy in path following was calculated. Next, mechanical properties of the tissue were calculated by using the tactile data and by assuming a viscoelastic behavior for the liver tissue. A finite element modeling (FEM) was also performed to investigate the reliability of the tactile data in tumor detection and experimental result's validation.

2. Material and Methods

2.1. Problem definition

Tumor shape identification and localization in the soft tissue are real challenges in the medical examinations and surgical operations. Moreover,

doctors are always looking for low cost methods for tumor identification. An automatic examination robot was designed to accurately examine the surface of soft tissue. The robot had to march the surface precisely in order not to miss any abnormalities. For such a purpose a number of paths were defined on the tissue surface and the robot was going to move on these paths. The robot was experimentally tested on a tissue phantom and outputs were validated with numerical modeling's results. For realistic simulation, mechanical properties of the tissue should be defined exactly.

2.2. Finite element modeling

Numerical modeling was done by using ABAQUS software (Release 6.14) based on a finite element approach. The tissue was considered as a cube with 60 mm width and the tumor as a pyramid, cube, and sphere with 8 mm diameter of their environmental sphere (Figure 1). Shape selection was based on the fact that vast majority of tumors have sharp edges and boundaries.

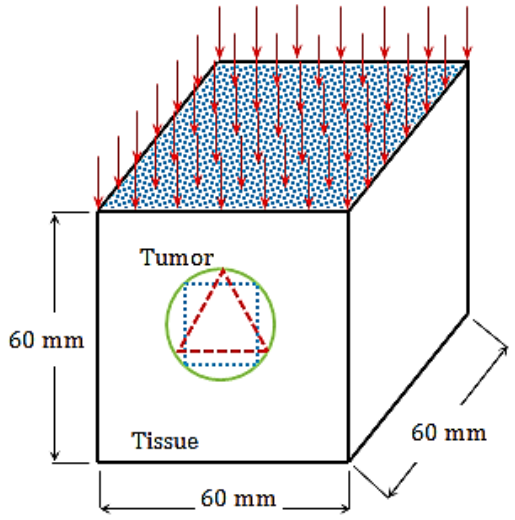

Figure 1. Schematic of liver tissue model including a pyramidal, a cuboid and a spherical tumor.

Mesh dependency was studied for the model, and 3.8% maximum error was achieved. For boundary conditions, side and bottom surfaces were fixed in the normal directions. In order to simulate tissue physical examination, a uniformly distributed load was applied on the upper surface of the tissue.

2.3. Viscoelastic modeling

For realistic modeling, soft tissue has to be considered as a viscoelastic body which has both rate-dependent and rate-independent properties. Rate-independent properties were defined by using a hyperelastic model:

$$\sigma_{hyperelastic} = \frac{\partial U}{\partial \varepsilon} \quad (1)$$

$$U = \sum_{i=1}^{N} C_{i0}(\bar{I}_1 - 3)^i + \sum_{i=1}^{N} \frac{1}{D_i}(J^{el} - 1)^{2i}, N = 2 \quad (2)$$

$$D_1 = \frac{2}{K_0} = \frac{3(1-2\upsilon)}{\mu_0(1+\upsilon)} \quad (3)$$

$$\mu_0 = 2C_{10} \quad (4)$$

Where in (1-4), I_1 is the first constant strain, J^{ei} is the ratio of elastic volume, N is the order of polynomial and the remaining coefficients (C_{i0},D_i) which corresponds to the initial shear modulus (μ_0), modulus of bulk (K_0), and Poisson's ratio (υ), are parameters of material. The model rate-dependency was obtained using model of viscoelastic material in ABAQUS, by definition of shear stress ($\tau(t)$) as:

$$\tau(t) = \int_0^t G_R(t-s)\dot{\gamma}(s)ds \quad (5)$$

Where in (5) $\dot{\gamma}$ is the rate of shear stress and $G_R(t)$ is the modulus of time dependent shear relaxation can be written in dimensionless form as:

$$g_R(t) = \frac{G_R(t)}{G_0} \quad (6)$$

Where in (6) G_0 is the modulus of instantaneous shear. The expansion of dimensionless relaxation modulus using Prony series is as (7).

$$g_R(t) = 1 - \sum_{k=1}^{M} \bar{g}_k^p(1 - e^{-t/\tau_k}) \quad (7)$$

Where in (7) M=2, and $\bar{g}_k^p$ and τ_k are constants of material. The function of strain energy (2) would be rederived by applying the coefficients of relaxation (8):

$$C_{i0}^R(t) = C_{i0}^0(1 - \sum_{k=1}^{M} \bar{g}_k^p(1 - e^{-t/\tau_k})) \quad (8)$$

2.4. Extracting mechanical properties

Mechanical properties were obtained from a set of experimental tests and were used as the inputs of the viscoelastic modeling. A particular robotic setup was implemented to extract the soft tissue mechanical properties through the relaxation (Figure 2) and uniaxial tests (Figure 3).

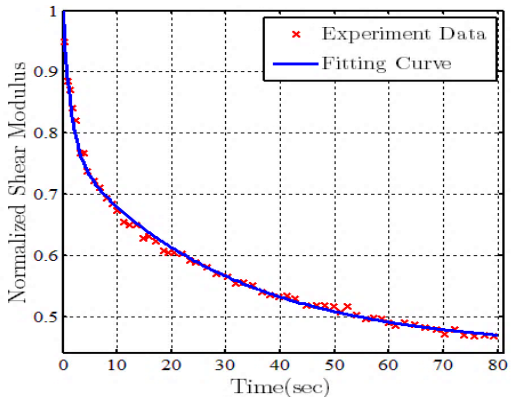

Figure 2. Shear relaxation test data extracted from experimental compression test [43].

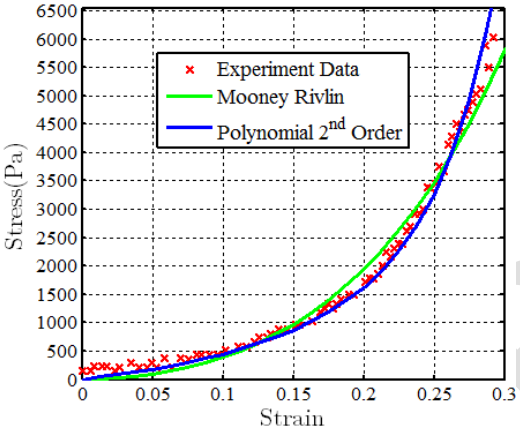

Figure 3. Uniaxial test data extracted from experimental compression test [43].

Viscoelastic coefficients were used as ABAQUS software input for the viscoelastic modeling. The coefficients were extracted from relaxation and uniaxial test data (Table 1 and Table 2). The stress-strain curve portion for the less than 10.5% strain was used to calculate the Young's modulus. Poisson's ratio of 0.45 was used for viscoelastic modeling in ABAQUS [43].

Table 1. The rate-independent material coefficients [43].

C_{10}^0	C_{20}^0	D_1	D_2
2.6×10^3	1.09×10^5	8.01×10^{-5}	0

Table 2. The rate-dependent material coefficients [43].

τ_1	τ_2	$\bar{g}_1^P$	$\bar{g}_2^P$
1.521	29.680	0.227	0.323

2.5. Robot specifications

For robotic examination of the liver tissue surface, an automatic examination robot was designed and fabricated (Figure 4). It basically consists of three prismatic joints and is classified as a Cartesian robotic mechanism. The axes of such mechanism are perpendicular to each other, forming X, Y and Z axes. The main advantage of using multiple linear Cartesian mechanisms is end-effector ability to move easily in three directions which provides easy access to the whole area of examination (Figure 5). Moreover, repeatability of the Cartesian mechanisms compared to SCARA or articulated arm is one of the plus points of this structure.

The automatic examination robot consists of three perpendicular ball screws (Lead size: 5 mm/Round; HIWIN; Taiwan) to produce linear movements driven by three DC motors (24 V; 110 RPM; Buhler; Germany). Speed of the linear motion is 55 cm/min. Three incremental rotary encoders (200 Pulse/Round) are able to detect position of the end-effector as an active feedback with respect to a predefined reference. In order to eliminate the impact of the backlash on position measurements, encoders are mounted on the other end of the ball screws instead of the motor shaft. According to the precision of 200 pulses per round for the encoders and the lead size of 5 mm per round for ball screws, every lead size of 5 mm can be divided to 200 parts. So the accuracy of position measurements would be equal to 25 microns.

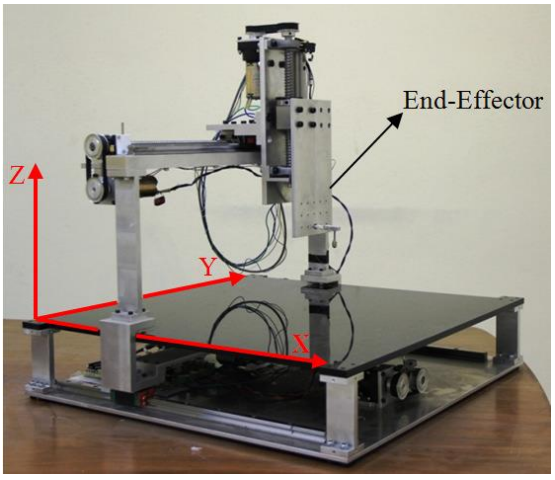

Figure 4. The automatic examiner robot fabricated for in vitro examinations.

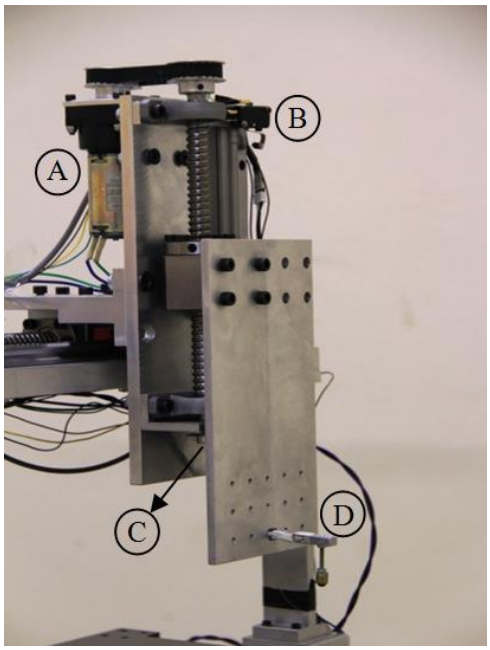

Figure 5. End-effector of the automatic examiner robot; A: DC Motor, B: Micro switch, C: Encoder, D: Probe.

Robot's workspace is a cube having 40 cm length, 40 cm width and 16 cm height. Any desirable trajectory needed to be traversed by the end effector should be defined in this workspace. The probe which is guided by the robotic mechanism is equipped with a pressure sensor. A freewheel is attached to the tip of the probe so that the entire tissue can be examined in a continuous and smooth pattern in the least possible time. To detect soft tissue abnormalities, an accurate sensor which is a beam load cell (Bongshin; South Korea) is used as shown in Figure 6. The load cell is suitable for measuring very low bending forces while it has 0.1% full scale linearity and hysteresis with an I65 range of environmental protection. The maximum measurable load by the sensor is 1 Kg. Voltage of 10 VDC is required for commissioning. The sensor's beam structure allows use of different probe shapes and sizes. Moreover, load cell is detailed enough to detect the exact touch point on the tissue surface. Touch point detection plays an important role in applying exact pattern of loading.

The entire system is controlled by an electronic board, which mainly includes: an 8 bit PIC18F65J50 processor (Microchip, USA) with 64KB RAM, 12MIPS processing speed, five PWM output with a 10bit resolution for driving 3 motors; a 32bit PIC32MX460F512L processor (Microchip, USA) as the main processor with 512KB RAM, 80MIPS processing speed and 5–stage pipeline structure; L298 IC for receiving the commands of PIC18F65J50 processor; a RS–232 industrial port with a 115200 bps baud rate which is used to connect the robot to computer; three 200 pulse shaft encoders with H9700 optical sensor for encoding the ball screws rotations; a 24 bit load cell with a HX711 analogue to digital IC; a switching power supply with 110/200 voltage input and 3.3/5/12/24 voltage output; a 74HC245 IC to decrease noise on the processors by buffering all the inputs and outputs signals; a unique PCB design for reducing noise of transferring data.

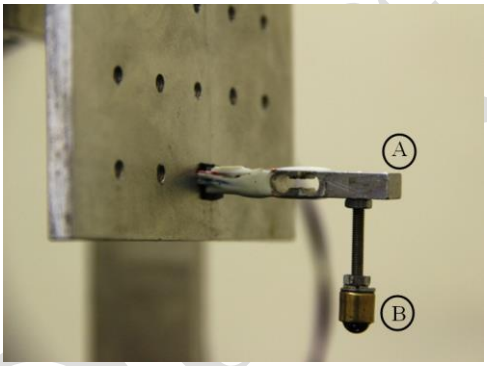

Figure 6. Tactile Sensing Probe of the automatic examiner robot; A: Beam Load Cell, B: Freewheel.

Board's microcontrollers' programming is done by compiler of the Microchip (MPLAB XC). The interaction between the operator and automatic examination robot is provided by MATLAB 8.3.0 (R2014a). This interaction provides the device's remote controlling feature. The device's output is received from the robot and is analyzed by software programming, MATLAB. The main target of such an interaction is increasing effectiveness and simple application of the robotic examination device.

2.6. Experimental protocol

Experimental tests by the robotic setup were made for tumor localization inside the liver tissue. Tests were done in terms of in vitro and sample tissue was selected through the following protocol. Fresh liver from local slaughterhouse was collected and refrigerated and applied at room temperature before tests. A piece of lamb liver in the form of a cylinder with 20mm diameter and 10mm height was cut and a special pattern of loading was applied by the robotic device. In order to simulate the embedded tumor, a solid sphere and a cube and pyramid with diameter of 8 mm of environmental sphere were placed inside the tissue sample. After preparation of the tissue sample, the automatic examination robot was used for in vitro examinations. For robotic examination the lamb liver sample was fixed by an aluminum clamp and the tissue center was aligned with the workspace center. The tip of the probe was placed exactly in contact with the surface to adjust the starting point of examination. The depth of compression for all examinations was selected to be 6 mm.

2.7. Path following

The end effector path was obtained through solving the inverse and forward kinematics. Analysis of the forward kinematic was straight forward, so the robot configuration in a space of joint could be uniquely mapped into an operational space. Inverse kinematics analysis could be solved to provide the end effector position and orientation with respect to a predefined origin.

An overall soft tissue scanning requires a precise path definition which could examine the whole tissue in the shortest possible time. Automatic examination robot was intended to follow a sinusoidal path and a step path. The paths were evaluated by a control system and robot accuracy in path following was calculated.

In the control system, sliding mode control (SMC) was implemented as a nonlinear control method which altered the dynamics of the nonlinear system by application of a discontinuous control signal. Such a signal forced the system to slide along the cross-section of the system's normal behavior. The state-feedback control law was not a continuous function of time. Instead, it could switch from one continuous structure to another based on the current position in the state space. The multiple control structure were designed in order to trajectories always move toward an adjacent region with a different control structure, and so the ultimate trajectory would not exist entirely within one control structure.

3. Results and Discussion

Examination result of the liver model containing a solid sphere tumor is shown in Figure 7a. The figure displays stress variation on the surface and inside the tissue. Stress elevation and also its gradients in the vicinity of tumor are noticeable. A straight path on the surface of the tissue over the tumor was defined. The path length was 60 mm and data collection was performed every 2 mm on the path. Tactile stress on the defined path is displayed in Figure 7b. It is worth to notice that while the peak is clearly indicative of tumor existence, such a graph is not an applicable common tool for a surgeon usage. A better visualization of the tissue examination is necessary.

Figure 8 is a 3D surface scan of the liver tissue. 3D stress plot provide a visual map of internal structure of the tissue. Each point on the map shows the stress amount of its corresponding point on the tissue surface. By means of such a 3D plot an embedded abnormality is easily detectable by the physician.

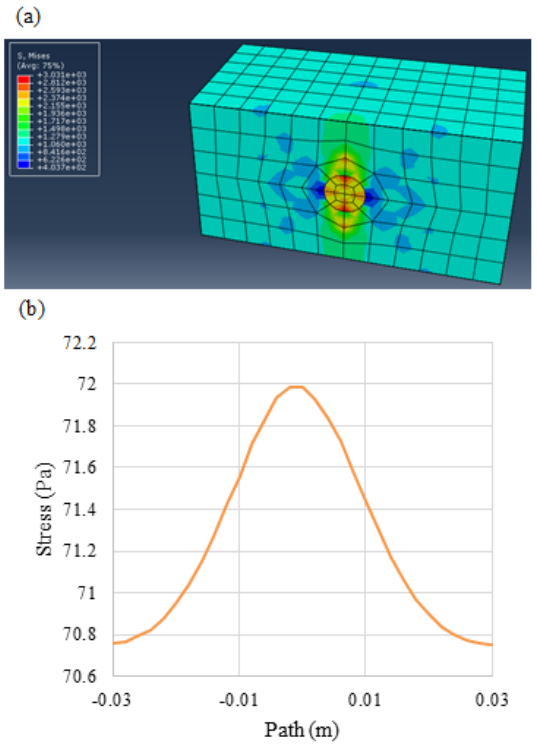

Figure 7. (a) Finite element model of liver tissue including an 8 mm diameter tumor, (b) Tactile stress on a straight path on the surface of the tissue over the tumor.

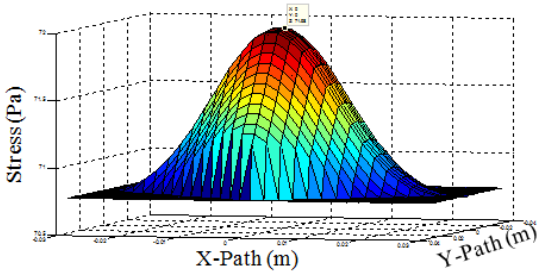

Figure 8. A through 3D numerical scan of the liver tissue model.

Interestingly, the 3D stress map of the tissue provides the surgeon with other information of the tumor rather than its presence. A number of geometrical features include tumor's location and boundary would be also achievable. It should be noted that tumor boundary is defined by its shape. In Figure 9, 3D stress contours related to three different geometrical tumor shapes are displayed together. It can be inferred that as the tumor shape becomes more irregular, smoothness of stress variations would be less.

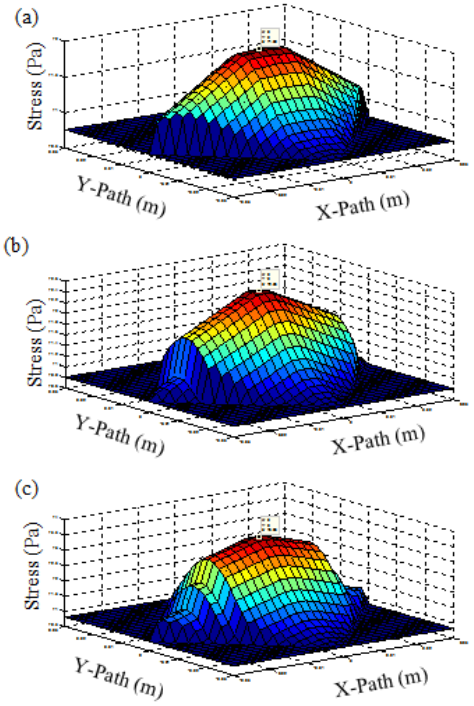

Figure 9. Peaks of the stress contour correspond to the geometrical shape of the embedded tumors; (a) pyramidal tumor, (b) cuboid tumor, (c) spherical tumor.

Numerical results proved the applicability of artificial tactile sensing in tumor detection embedded inside a soft tissue. The same procedure was conducted by the automated examination robot and the achieved experimental results were compared with the corresponding numerical ones. Experimental and numerical examination results on a 6 mm diameter sphere tumor are shown in Figure 10. It is palpable that the maximum stress achieved by the robotic examination is very close to the FEM results. Moreover, overshoot's coordinate in the experimental stress curve coincides with the peak of the stress diagram in FEM.

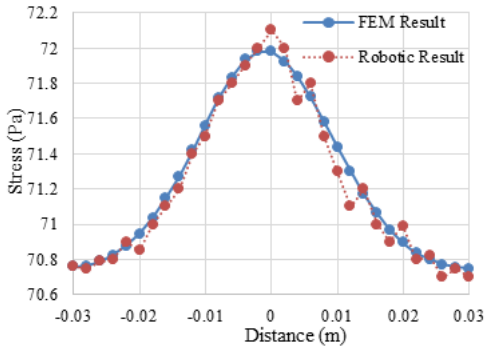

Figure 10. Robotic tactile result in comparison with FEM result.

One of the most important robot performance evaluations is to ensure that the robot can follow the user's desired path. The end effector path following accuracy was investigated through the two desired path design followed by robot (Figure 11 and Figure 12). The automatic examination robot mean error in path following task for sinusoidal path and step path were 3.26% and 0.76%, respectively, which shows the Cartesian mechanism high accuracy and reliability in soft tissue scanning. Using Cartesian motion mechanism and optimal design of sliding mode controller, the significant performance of the robot in pursuit of the desired path and tissue abnormality detection was achieved.

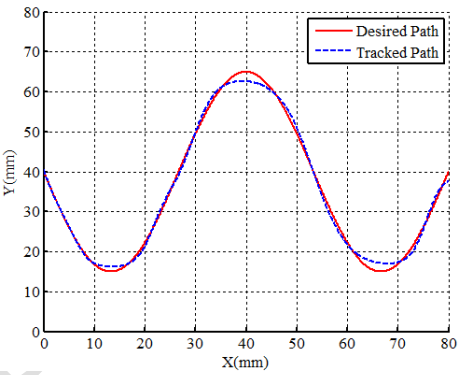

Figure 11. Path following by the end effector of the automatic examiner robot for a sinusoidal path.

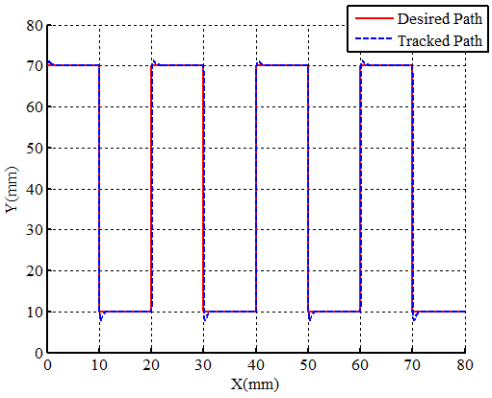

Figure 12. Path following by the end effector of the automatic examiner robot for a step path.

4. Conclusion

In this paper, we extracted viscoelastic coefficients of a lamb liver tissue by implementing an automatic examination robot. The robot was equipped with a palpation probe and a pressure sensor. The extracted coefficients were used in FEM modeling and the ability of robot in tumor detection was confirmed. The experimental results showed that tumor detection and localization would be more accurate and more reliable by using an examination robot instead of the physician's palpation. Moreover, ability of path

following by the robot eventuated to powerful tumor localization. The future studies target is to investigate the influence of depth and diameter of tumor in robotic assisted tumor detection. Furthermore the robot examination path can be optimized in order to minimize the examination time.

References

[1] M. Naghavi, H. Wang, R. Lozano, A. Davis, X. Liang, M. Zhou, S.E. Vollset, A.A. Ozgoren, S. Abdalla, F. Abd-Allah and et al, Global, regional, and national age-sex specific all-cause and cause-specific mortality for 240 causes of death, Lancet, 385 (2015) 117-171.

[2] F. Xavier Bosch, J. Ribes, M. Diaz, R. Cleries, Primary liver cancer: Worldwide incidence and trends. Gastroenterology, 127 (2004) 5-16.

[3] http://www.cancer.org © 2015 American Cancer Society, Inc.

[4] H.O. Yegingil, Breast cancer detection and differentiation using piezoelectric fingers, PhD diss., Drexel University, (2009).

[5] M Kaufmann, G von Minckwitz, R.Smith, et al. International expert panel on the use of primary (preoperative) systemic treatment of operable breast cancer: review and recommendations, JClinOncol, 21 (2003) 2600–2608.

[6] A. Mojra, S. Najarian, S.M. Towliat Kashani, F. Panahi, A novel tactile-guided detection and three-dimensional localization of clinically significant breast masses, Journal of medical engineering & technology, 36, no. 1 (2012) 8-16.

[7] A.P. Sarvazyan, Knowledge-based mechanical imaging, In Computer-Based Medical Systems, 1997. Proceedings, Tenth IEEE Symposium on, pp. 120-125. IEEE, (1997).

[8] S. Najarian, M. Fallahnezhad, E. Afshari, Advances in medical robotic systems with specific applications in Surgery – A Review, J Med Eng Technol, 35 (2011) 13-19.

[9] R.D. Howe, Tactile sensing and control of robotic manipulation. Adv Robot, 8 (1994) 245–261.

[10] G. Riva, L. Gamberini, Virtual reality in telemedicine, communication through virtual technology, ISO Press Amsterdam, 2003.

[11] R.D. Howe, W.J. Peine, D.A. Kontarinis, J.S. Son, Remote palpation technology, IEEE Engineering in Medicine and Biology, 3 (1995) 18–23.

[12] P. Dario, M.C. Carrozza, L. Lencioni, B. Magnani, S. D'Attanasio, A micro robot system for colonoscopy, Proceedings of the IEEE International Conference on Robotics and Automation, (1997) 1567–1572.

[13] Y. Murayama, C.E. Constantinou, S. Omata, Development of tactile mapping system for the stiffness characterization of tissue slice using novel tactile sensing technology, Sensors and Actuators A-Physical, 120 (2005) 543–549.

[14] J. Dargahi, S. Najarian, An endoscopic force position grasper with minimum sensors, Can J Electr Comput Eng, 28 (2003) 155–161.

[15] J.R. Harris, M.E. Lippman, M. Morrow, S. Hellman, Diseases of the breast, Lippincott-Raven: 1996.

[16] L. Han, M. Burcher, J.A. Noble, Non-invasive measurement of biomechanical properties of in vivo soft tissues, MICCAI 2002 LNCS, 2488 (2002) 208–215.

[17] C.S. Kaufman, L. Jacobson, B.A. Bachman, L.B. Kaufman, Digital documentation of the physical examination: moving the clinical breast exam to the electronic medical record, The American journal of surgery, 192(4) (2006) 444-449.

[18] S. Schostek, M.J. Binser, F. Rieber, C.N. Ho, M.O. Schurr, G.F. Buess, Artificial tactile feedback can significantly improve tissue examination through remote palpation, Surgical endoscopy, 24(9) (2010) 2299-2307.

[19] T. Hoshi, Y. Kobayashi, T. Miyashita, M.G. Fujie, (2010, October), Quantitative palpation to identify the material parameters of tissues using reactive force measurement and finite element simulation, In Intelligent Robots and Systems (IROS), 2010 IEEE/RSJ International Conference on (pp. 2822-2828). IEEE.

[20] F.J. Carter, T.G. Frank, P.J. Davies, D. McLean, A. Cuschieri, Measurements and modelling of the compliance of human and porcine organs, Medical Image Analysis, 5(4) (2001) 231-236.

[21] H. Liu, D.P. Noonan, K. Althoefer, L.D. Seneviratne, (2008, May), Rolling mechanical imaging: a novel approach for soft tissue modelling and identification during minimally invasive surgery, In Robotics and Automation, 2008, ICRA 2008, IEEE International Conference on (pp. 845-850), IEEE.

[22] P.L. Yen, D.R. Chen, K.T. Yeh, P.Y. Chu, Lateral exploration strategy for differentiating the stiffness ratio of an inclusion in soft tissue. Medical engineering & physics, 30(8) (2008) 1013-1019.

[23] M. Ayyildiz, B. Guclu, M.Z. Yildiz, C. Basdogan, A novel tactile sensor for detecting lumps in breast tissue, In Haptics: Generating and Perceiving Tangible Sensations (pp. 367-372) (2010) Springer Berlin Heidelberg.

[24] J.H. Lee, C.H. Won, K. Yan, Y. Yu, L. Liao,, Tactile sensation imaging for artificial palpation, In Haptics: Generating and Perceiving

Tangible Sensations (pp. 373-378) (2010) Springer Berlin Heidelberg.

[25] M.P. Ottensmeyer, Minimally invasive instrument for in vivo measurement of solid organ mechanical impedance, Massachusetts Institute of Technology, 2001.

[26] J. Dargahi, R. Sedaghati, H. Singh, S. Najarian, Modeling and testing of an endoscopic piezoelectric-based tactile sensor, Mechatronics, 17(8) (2007) 462-467.

[27] A. Mojra, S. Najarian, S. M. Towliat Kashani, F. Panahi, M. Yaghmaei, A novel haptic robotic viscogram for characterizing the viscoelastic behaviour of breast tissue in clinical examinations, The International Journal of Medical Robotics and Computer Assisted Surgery, 7(3) (2011) 282-292.

[28] C. Ledermann, H. Alagi, H. Woern, R. Schirren, S. Reiser, Biomimetic tactile sensor based on Fiber Bragg Gratings for tumor detection—Prototype and results, pp. 1-6.

[29] G. H. Büscher, R. Kõiva, C. Schürmann, R. Haschke, H. J. Ritter, Flexible and stretchable fabric-based tactile sensor, Robotics and Autonomous Systems, 63 (2015) 244-252.

[30] A. Mojra, S. Najarian, S.M. Hosseini, S.M. Towliat Kashani, F. Panahi, Abnormal Mass Detection in a Real Breast Model: A Computational Tactile Sensing Approach, World Congress on Medical Physics and Biomedical Engineering, 25 (2009) 115-118.

[31] A. Mojra, S. Najarian, S.M. Towliat Kashani, F. Panahi , Artificial Tactile Sensing Capability Analysis in Abnormal Mass Detection with Application in Clinical Breast Examination, World Congress on Engineering, 3 (2011).

[32] A. Mojra, S. Najarian, S.M. Towliat Kashani, F. Panahi, M. Ali Tehrani, A novel robotic tactile mass detector with application in clinical breast examination, Minimally Invasive Therapy & Allied Technologies, 21 (2012) 210-221.

[33] Y. Kim, B. Ahn, Y. Na, T. Shin, K. Rha, J. Kim, Digital rectal examination in a simulated environment using sweeping palpation and mechanical localization. International Journal of Precision Engineering and Manufacturing, 15 (2014) 169-175.

[34] A.A. Wahba, N.M.M. Khalifa, A.F. Seddik, M.I. El-Adawy, A Finite Element Model for Recognizing Breast Cancer, Journal of Biomedical Science and Engineering, 7 (2014).

[35] A.P. Astrand, V. Jalkanen, B.M. Andersson, O.A. Lindahl, Detection of Stiff Nodules Embedded in Soft Tissue Phantoms, Mimicking Cancer Tumours, Using a Tactile Resonance Sensor, Journal of Biomedical Science and Engineering, 7 (2014).

[36] Y.B. Fu, C.K. Chui, C.L. Teo, E. Kobayashi, Elasticity imaging of biological soft tissue using a combined finite element and non-linear optimization method, Inverse Problems in Science and Engineering, 23 (2014) 179-196.

[37] M. Heverly, P. Dupont, J. Triedman, Trajectory Optimization for Dynamic Needle Insertion, Robotics and Automation, (2005) 1646-1651.

[38] D. Valtorta, E. Mazza, Dynamic measurement of soft tissue viscoelastic properties with a torsional resonator device, Medical Image Analysis, 9 (2005) 481-490.

[39] H. Shi, A. Farag, Validating linear elastic and linear viscoelastic models of lamb liver tissue using cone-beam CT, International Congress Series, 1281 (2005) 473-478.

[40] M. Zhang, B. Castaneda, Z. Wu, P. Nigwekar, J.V. Joseph, D.J. Rubens, K.J. Parker, Congruence of Imaging Estimators and Mechanical Measurements of Viscoelastic Properties of Soft Tissue, Ultrasound in Medicine & Biology, 33 (2007) 1617-1631.

[41] Y. Kobayashi, A. Onishi, T. Hoshi, K. Kawamura, M. Hashizume, M.G. Fujie, Development and validation of a viscoelastic and nonlinear liver model for needle insertion, International Journal of Computer Assisted Radiology and Surgery, 4 (2009) 53-63.

[42] S. Raghunathan, D. Evans, J.L. Sparks, Poroviscoelastic Modeling of Liver Biomechanical Response in Unconfined Compression, Annals of Biomedical Engineering, 38 (2010) 1789-1800.

[43] I. Sakuma, Y. Nishimura, C.K. Chui, E. Kobayashi, H. Inada, X. Chen, T. Hisada, In vitro measurement of mechanical properties of liver tissue under compression and elongation using a new test piece holding method with surgical glue, Surgery Simulation and Soft Tissue Modeling, 2673 (2003) 284-292.

Biography

Ms. Afsaneh Mojra has obtained her BSCE degree in Mechanical Engineering from Sharif University of Technology, Tehran, Iran in 2004, her MSC in Biomedical Engineering from Amirkabir University of Technology (Tehran Polytechnic), Tehran, Iran in 2006 and her PHD in Biomedical Engineering from Amirkabir University of Technology (Tehran Polytechnic), Tehran, Iran in 2011. She has spent a sabbatical position in the Biomedical Department, Eindhoven University of Technology, Netherlands in 2010. She is now an assistant professor in K. N. Toosi University of

Technology in the Mechanical Engineering Department.

Mr. Seyed Mohammad Salman Lari is now a BSC student in Mechanical Engineering in K. N. Toosi University of Technology, Tehran, Iran.